Korean J. Chem. Eng., 35(9), 1791-1799 (2018)
DOI: 10.1007/s11814-018-0093-x

pISSN: 0256-1115
eISSN: 1975-7220

Modeling and simulation for acrylamide polymerization of super absorbent polymer

Gun Hee Lee*, Nguyen Dat Vo*, Rak Young Jeon*, Seung Whan Han, Seong Uk Hong*,†, and Min Oh*,†**

*Department of Chemical and Biological Engineering, Hanbat National University,
Dongseo-daero 125, Yuseong-gu, Daejeon 34158 Korea
**Department of Biology, Adelphi University, 1 South Ave, 701, Garden City, New York 11530-0701, United States
(*Received 24 February 2018 • accepted 4 June 2018*)

Abstract−In view of the scale up of a batch reactor for super absorbent polymer (SAP), a dynamic mathematical model of a commercial scale batch reactor was developed with mass balance, energy balance, and complex polymerization kinetics. The kinetic parameters of the polymerization were estimated on the basis of the established mathematical model and reference data. Simulation results were validated with less than 10% marginal error compared with reference data. A case study was executed in terms of dynamic simulation for eight different initial concentrations of initiator and monomer to analyze the influence of initial concentration and predict the operation condition for desired product. The results were compared with various reference data, and good agreement was achieved. From the results, we argue that the methodology and results from this study can be used for the scale up of a polymerization batch reactor from the early stage of design.

Keywords: Super Absorbent Polymer, Polyacrylamide, Parameter Estimation, Dynamic Simulation, Batch Reactor

INTRODUCTION

Some materials that can absorb water in daily life are filter paper, cosmetic tissues, and sponges. The absorption capacity of these materials is only several times their own weight while the absorbed water is easily released under pressure. Super absorbent polymer (SAP), which is a synthetic polymeric substance, can absorb huge amounts of water compared to its own weight [1,2]. According to a recent study, 1 g SAP has the ability to absorb about 1,000 g of water [3]. A typical advantage of SAP is its good retention of absorbed water even under applied pressure, owing to its cross-linked structure [4]. About 90% of SAP has been used in hygiene products (diapers). Other applications include packaging materials, pharmaceutics, cosmetic, oil recovery, agriculture and environment protection [5,6]. On account of an aging society and the improvement of the world's income levels among developing countries in Africa, China, and South America, the demand for diapers for adults and infants has rapidly increased. Accordingly, the research on the development of high quality SAP has gained strong attention.

Despite the importance of SAP research results, process simulation has seldom been reported in open literature due to the nature of SAP production classified as a company's property. Researches on SAP have mainly focused on the absorption and swelling capacity of polyacrylamide for application [7-11]. There have been few studies regarding the mechanism, reaction kinetics and simulation for polymerization of SAP in batch reactor up to now. The researches for polymerization of SAP can be classified into experimental studies and modeling and simulation studies.

Ishige's research group carried out the experiment for the polymerization of acrylamide on lab scale with the initiator 4,4′-azobis-4-cyanovaleric acid [12]. This author estimated the kinetic parameters and predicted the polymer properties under isothermal condition. Also, the mechanism and kinetics of polymerization of acrylamide were studied on the lab scale with potassium persulfate initiator [13,14,22-24]. These authors suggested the relation between rate constants of decomposition, initiation, propagation and termination steps without the derivation of activation energy and frequency factor. Therefore, this information is not enough for simulation, especially in the case of persulfate compound initiator.

The kinetic parameters for polymerization of acrylamide with initiator 2,2-azobisdihydrochloride were also studied and predicted polymer properties under isothermal condition [15]. The isothermal polymerization of acrylamide was also studied by using the kinetic model for different initiators to estimate the kinetics parameters and to predict the polymer properties [12,25]. These authors just focused on the development of the mass conservation to predict the kinetic parameters for different initiators. However, the reactor temperature cannot be kept constant always in real operating condition, especially with polymerization. Therefore, energy conservation is necessary for the modeling and simulation to predict the dynamic polymer properties. As a result, the gap in terms of kinetic parameters for polymerization with the persulfate initiator and the demand of energy conservation are the motivation of this study.

A commercial scale batch reactor was the target process for modeling and simulation in our research. The species conservation equations were established based on the mechanism of acrylamide polymerization for all stages. Kinetics parameters were estimated by maximum likelihood method on the basis of reference experimental data. Moreover, cooling jacket with PI controller model was

†To whom correspondence should be addressed.
E-mail: minoh@hanbat.ac.kr, suhong@hanbat.ac.kr

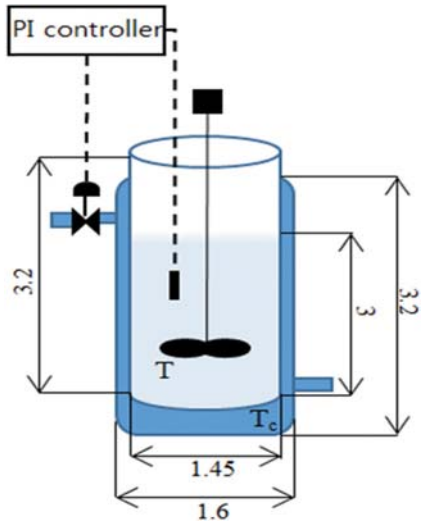

Fig. 1. Schematic of the batch reactor for the polymerization of SAP.

established to control the reactor temperature. Process simulation was carried out to find the proper operation not only to achieve the properties of polyacrylamide in terms of Mn, Mw, MWD, and PD, but also to reduce the reaction time for various feed conditions. The *gPROMS* modelling package [16] was utilized as a software platform for modeling and simulation.

FORMULATION OF A PROBLEM

1. Process and Mathematical Description

The batch reactor for the SAP production, shown in Fig. 1, is a stirred reactor surrounded by a cooling jacket to remove the heat of polymerization and to control the reactor temperature. The PI controller was used to control the reactor temperature by controlling the inlet flow rate of chilled water (7 °C) in the cooling jacket.

Initial components include acrylamide (monomer), potassium persulfate (initiator), and water. Since good mixture is assumed, the state variables (concentration, temperature, density, etc.) are equal at any points inside the reactor. Therefore, the batch reactor was modelled as a lumped parameter system with zero dimension.

1-1. Polymerization Reactor

The mass and energy conservation equations were used to calculate the time transient of concentration and reactor temperature.

Mass conservation

$$\frac{dc_i}{dt} = \hat{s}_m^i \tag{1}$$

$$\hat{s}_m^i = \sum \gamma_{ji} r_j^i, \text{ with J = D, I, P, T} \tag{2}$$

where, D: decomposition, I: Initiation, P: Propagation, T: Termination

Eq. (2) shows the rate of creation and disposition of the i^{th} component during polymerization. Here, the reaction rate (r_j^i) is shown in Table 1, the reaction order (γ_{ji}) gets a plus value for product and minus value for reactant.

Table 1. Reaction mechanism and reaction rate for acrylamide polymerization [12]

	Mechanism	Reaction rate
Decomposition	$I \xrightarrow{k_D} 2R_c^{\cdot}$	$r_D = k_D[I]^{0.5}$
Initiation	$R_c^{\cdot} + M \xrightarrow{k_I} R_1^{\cdot}$	$r_I = k_I[R_c^{\cdot}][M]^{1.25}$
	$R_1^{\cdot} + M \xrightarrow{k_P} R_2^{\cdot}$	
Propagation	$R_2^{\cdot} + M \xrightarrow{k_P} R_3^{\cdot}$	$r_{P_j} = k_P[R_j^{\cdot}][M]^{1.25}$
	$\vdots$	
	$R_r^{\cdot} + M \xrightarrow{k_P} R_{r+1}^{\cdot}$	
Termination	$R_r^{\cdot} + R_s^{\cdot} \xrightarrow{k_T} P_r + P_s$	$r_T = k_T[R_r^{\cdot}][R_s^{\cdot}]$

Energy conservation

$$\rho \hat{C}_p \frac{dT_R}{dt} = s_e - \frac{\dot{q}}{v} \tag{3}$$

$$\hat{s}_e = \left(r_D + r_I + \sum_{j=1}^{j=n} r_{P_j} + r_T \right) h_p \tag{4}$$

Eq. (3) was developed based on the energy conservation equation. Here, the accumulated energy ($\rho \hat{C}_p$ (dT_R/dt)) is equal to the minus of heat source from reactions in polymerization ($\hat{s}_e$) to heat transfer from reactor to cooling jacket ($\dot{q}/v$). Because of the limitation of heat formation of components in polymerization, we used the heat of polymerization for all steps. Therefore, the heat source of polymerization is the multiple of the total reaction rate and heat of polymerization as in Eq. (4).

1-2. Cooling Jacket

Mass conservation

$$\frac{dm_c}{dt} = \dot{m}_c^{in} - \dot{m}_c^{out} \tag{5}$$

$$\dot{m}_c^{in} = K_c \left(\varepsilon(t) + \frac{1}{\tau_I} \int \varepsilon(t) dt \right) + C_s \tag{6}$$

$$\varepsilon(t) = T_{SP} - T_R \tag{7}$$

Energy conservation

$$m_c \hat{C}_{Pc} \frac{dT_c}{dt} = \dot{m}_c^{in} \hat{h}_c^{in} - \dot{m}_c^{out} \hat{h}_c^{out} + \dot{q} \tag{8}$$

Heat transfer with reactor

$$\dot{q} = UA_{h,t}(T_R - T_c) \tag{9}$$

$$U = \frac{1}{R_t A_{h,t}} \tag{10}$$

$$R_t = R_t^{cond} + R_t^{conv} \tag{11}$$

$$R_t^{cond} = \frac{\ln(r_c/r)}{2\pi L k_d} \tag{12}$$

$$R_t^{conv} = \frac{1}{hA_{h,t}} \tag{13}$$

Polymer properties

The characteristic properties of polyacrylamide identified in this research include number/weight average molecular weight, polydis-

persity index (PD), and molecular weight distribution.

Number average molecular weight: Mn

$$Mn = \sum_{i=1}^{n} \frac{c_i^p}{c_{total}^p} M_i \quad (14)$$

$$c_{total}^p = \sum_{i=1}^{n} c_i^p \quad (15)$$

Weight average molecular weight: Mw

$$x_i = \frac{c_i^p}{\sum_{i=1}^{n} c_i^p} \frac{M_i}{Mn} \quad (16)$$

$$Mw = \sum_{i=1}^{n} x_i M_i \quad (17)$$

Polydispersity index: PD

$$PD = \frac{Mw}{Mn} \quad (18)$$

The numerical solution of the mathematical model is shown in Fig. 2 above. In this study, the polymerization was simulated based on the discretization and integration methods. The discretization in gPROMS was carried out by assigning different integers to each component. The integration was defined by the sigma function in gPROMS to calculate the sum of variable over the defined domain, and then used to estimate the polymer properties. After the discretization and integration, our mathematical model became a set of differential algebraic equations (DAEs). The DAEs were solved by the same algorithm as with our previous publications [17,18]. DAEs were numerically integrated with solution algorithm based on backward differential formula (BDF) method. During the integration, linear algebraic equations (LAEs) and nonlinear algebraic equations (NAEs) were formulated and solved by the quasi-Newton method and LA solution method. For convergence, absolute and relative tolerances of 10^{-5} were used.

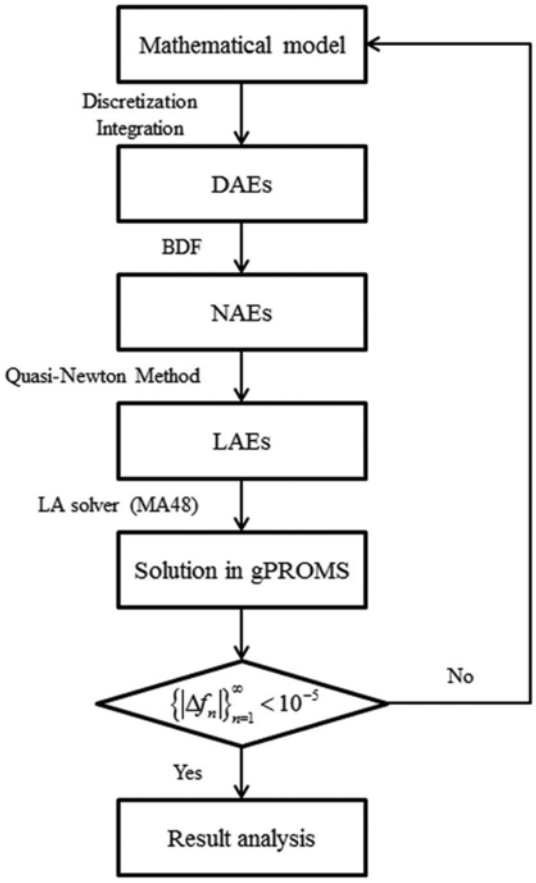

Fig. 2. The numerical solution of the mathematical model.

2. Polymerization Kinetics

SAP is synthesized by free radical polymerization and polymer is rapidly generated after initiation. A detailed mechanism for the radical polymerization reaction in a batch reactor is shown in Table 1. This involves decomposition, initiation, propagation, and termination steps. The termination by combination can be neglected because disproportionation is predominant [19]. Based on the study by Nedal Y.Abu-Thabit [20], we used the heat of polymerization with the value of 18 Cal/mol.

Previous studies [13,14,22-24] determined the kinetics values as the constant and the ratio between each rate constants at various temperature conditions without deriving for activation energy and frequency factor in Arrhenius equation as shown in Table 2.

However, this information is not sufficient to execute process simulation due to lack of kinetic constant for initiation, as well as the exact kinetics of propagation and termination. In addition, considering polymerization is sensitive to temperature, temperature dependency of reaction parameters should be deliberated. In this study, the kinetics parameters of initiation and propagation were estimated by using the parameter estimation function in *gPROMS*, while the kinetics parameter of termination was determined from

Table 2. Kinetic parameters for acrylamide polymerization [13]

	Kinetic parameters		
T [K]	343	333	323
k_D [1/s]	8.75e-6	3.78e-6	9.8e-7
k_p^2/k_T [L/Ms]	16.7±0.95	14.7±1.05	10.6±1.5

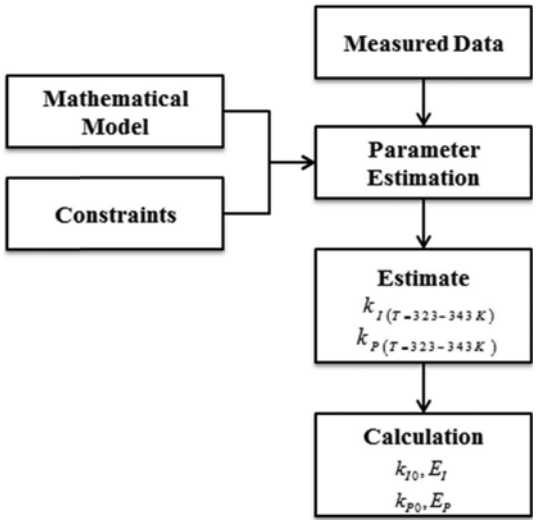

Fig. 3. Parameter estimation procedure.

the ratio of propagation and termination as shown in Table 2.

Maximum likelihood method [16] was employed to calculate reaction parameters to minimize the possibility of errors between the measured conversion and the predicted conversion. The whole procedure of parameter estimation is summarized in Fig. 3.

The rate constants for reaction j are expressed by Arrhenius Eq. (19), and our target was to obtain $k_{j,o}$ and E_j for initialization and propagation.

$$k_j = k_{j,o}\exp\left(-\frac{E_j}{RT_R}\right),\ j = I,\ P \tag{19}$$

$$X_{ij} = \frac{c_{M_{ij}}}{c_{M\_initial}} \tag{20}$$

$$\min_{\theta}\left\{\sum_{i=1}^{NE}\sum_{j=1}^{NM_i}\left[\ln(\sigma_{ij}^2) + \frac{(X_{ij}-\tilde{X}_{ij})^2}{\sigma_{ij}^2}\right]\right\} \tag{21}$$

subject to

$$T_l \le T_{reactor} \le T_h$$

Equation (1)-(15) (22)

$$\sigma_{ij}^2 = \omega^2(\tilde{X}_{ij}^2 + \varepsilon)$$

The experimental data, such as conversion, were used as measured values. The parameters were estimated to minimize the error between the predicted conversion (X_{ij}) and measured conversion ($\tilde{X}_{ij}$) as shown in Eq. (21). Additionally, the parameter estimation should consider operational limitations (e.g., reactor temperature) and physicochemical phenomena occurring in the reactor, described by the mathematical model. These led to the introduction of constraints, which were denoted by Eq. (22).

Parameters were estimated with the conditions of the standard deviation being lower than the optimal estimate and the 95% t-value being higher than the reference t-value (95%) [16]. The kinetic parameter values obtained from parameter estimation are shown in Table 3.

The estimated values of 95% t-value of initiation and propagation at 323 K, 333 K, and 343 K are higher than the recommended reference of 95% t-value (1.69). Calculated standard deviation values are also much lower than the recommended range for accurate parameter estimate (from a range of 8 to 18 times) [16,21]. The kinetics parameter values are close to the result of other researches [22,23]. Therefore, the kinetic parameter values obtained from parameter estimation are acceptable.

The kinetic parameter values from the simulation were com-

Table 3. Kinetic parameter values from parameter estimation

Parameter	Optimal estimate	95% T-value	Standard deviation
$k_I(323)$	3.66e-6	4.600	2.08e-7
$k_I(333)$	9.31e-6	3.660	8.13e-7
$k_I(343)$	2.22e-5	4.154	2.04e-6
$k_{I,0}$	1.18e8		
E_I	83532		
$k_P(323)$	1.34e-2	5.400	1.79e-3
$k_P(333)$	2.31e-2	6.634	3.1e-3
$k_P(343)$	3.85e-2	4.003	4.53e-3
$k_{P,0}$	9e5		
E_P	48386		

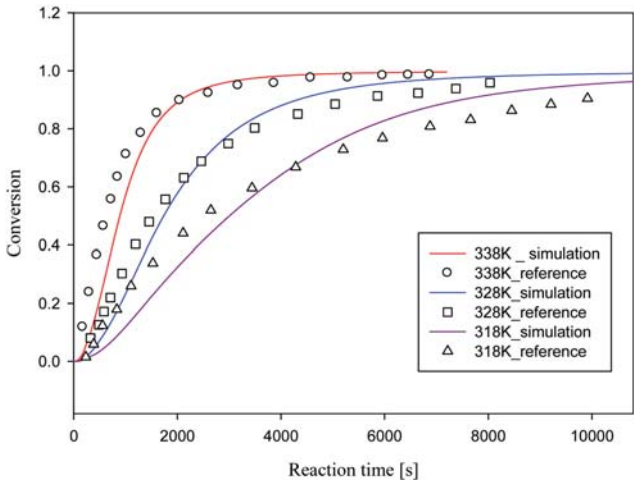

Fig. 4. Comparison of the conversion between simulation and reference data [24]: [AM]=700 mol/m^3; [I]=2.25 mol/m^3; T=318, 328, 338 K.

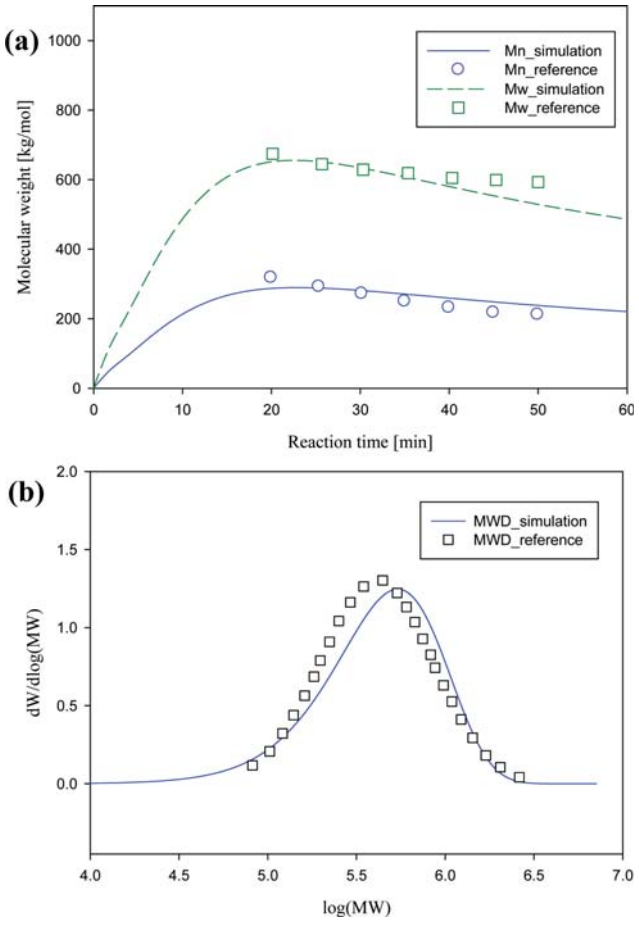

Fig. 5. Comparison of the average molecular weight and molecular weight distribution between simulation and reference data [25]: [AM]=250 mol/m^3; [I]=5 mol/m^3; T=340 K.

pared to other reference data [24,25] with respect to the monomer conversion and polymer properties, and the results are shown in Fig. 4 and Fig. 5.

Fig. 4 demonstrates the conversion profile between the simulation results and reference data [24] with the operation conditions of monomer concentration ([AM]) at 700 mol/m^3; initiator concentration ([I]) at 2.25 mol/m^3 and reactor temperatures at 318, 328 and 338 K. With increasing the reactor temperature, the simulation results had the same tendency with reference data due to the relation between rate constant and reactor temperature in Eq. (14). There was plausible agreement between them with the marginal difference.

Fig. 5 illustrates the molecular weight profile of the simulation results and reference data [25] with the operation conditions of monomer concentration ([AM]) at 250 mol/m^3; initiator concentration ([I]) at 5 mol/m^3 and reactor temperature at 340 K.

The number and weight average molecular weights achieved the same tendency, in which their values decreased with the increase of time due to the formulation of smaller polymer chain. The maximum error of simulation results for number and weight average molecular weights was less than 10% range compared with reference data. Meanwhile, the molecular weight distribution of simulation was similar to the diagram of reference [25]. From the acceptable validation between simulation and reference, kinetics parameter values have been used for case study.

3. Simulation Basis

Design and operating conditions for simulation are illustrated in Table 4. The reactor dimensions were chosen based on the desired capacity (5 m^3), and the standard ratio of diameter and height was 0.5.

Polyacrylamide manufacturers have normally used the concentration ratio of initiator and monomer in the range of 0.1 to 0.0035 [13,26].

Initiator effects were simulated with the change of initiator concentration when the monomer concentration was of a fixed value or 500 mol/m^3 (M1, M2, M3, M4). To evaluate monomer effects on conversion and polymer properties, simulation was executed, with the change of the monomer concentration as the initiator concentration being 4.00 mol/m^3 (I1, I2, I3, I4).

RESULTS AND DISCUSSION

1. Conversion

Fig. 6 displays the transient conversion of monomer at various simulation conditions as shown in Table 5.

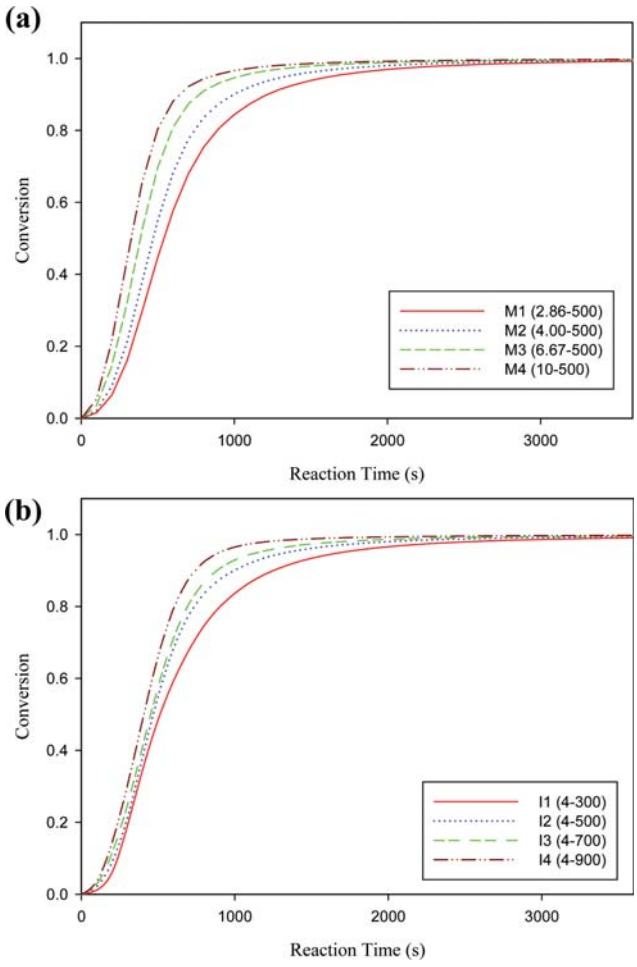

Fig. 6. Transient monomer conversion profiles: (a) with fixed monomer and various initiator concentrations (M1, M2, M3, M4) and (b) with fixed initiator and various monomer concentrations (I1, I2, I3, I4).

As shown in Fig. 6(a), when the initiator concentrations are 2.86 mol/m^3 (M1), 4.00 mol/m^3 (M2), 6.67 mol/m^3 (M3), and 10 mol/m^3 (M4), the conversions become 0.9 at t=1180 s, 996 s, 773 s, and 646 s, respectively. Since the reaction rate of decomposition is

Table 4. Design and operating basis for modeling and simulatio

Parameter	Value
Height of reactor [m]	3.2
Diameter of reactor [m]	1.45
Feed volume [m^3]	5
Diameter of jacket [m]	1.6
Flowrate of chilled water [kg/s]	0.01-10
Initial temperature of reactor [K]	343.15
Initial temperature of cooling jacket [K]	280.15
Pressure [kPa]	101,325

Table 5. Case studies for the simulation of acrylamide polymerization

Case no.	Initiator [mol/m^3]	Monomer [mol/m^3]	Molar ratio (Persulf/Am)
M1	2.86	500	0.0057
M2	4.00	500	0.008
M3	6.67	500	0.0133
M4	10	500	0.02
I1	4.00	300	0.0133
I2	4.00	500	0.008
I3	4.00	700	0.0057
I4	4.00	900	0.0044

proportional to the initiator concentration, decomposition rate increases with the increasing initiator concentration, as reported by a similar work [26]. Therefore, the reaction rates of initiation and propagation become higher because they are proportional to the concentration of intermediate product (R_c) that is created in the decomposition step. Accordingly, the higher the initiator concentration, the faster the conversion.

Also, as shown in Fig. 6(b), when the monomer concentrations (at the same initiator concentration) are 300 mol/m^3 (I1), 500 mol/m^3 (I2), 700 mol/m^3 (I3) and 1,000 mol/m^3 (I4), the conversions become 0.9 at t=1260 s, 996 s, 886 s, and 748 s, respectively. As expected, for higher monomer concentration, a faster conversion rate can be achieved. This tendency agrees well with the experimental results of other researchers [27]. Accordingly, it is proper to conclude that the reaction time can be reduced by increasing the concentration of the initiator and monomer.

2. Temperature Profile

Since acrylamide polymerization is the exothermic reaction, the reactor temperature is increased rapidly during polymerization. As discussed earlier, kinetic constants are a strong function of temperature, and temperature control plays an important role to maintain the reactor temperature to produce the desired product by the inlet flow rate of chilled water. Reactor temperature was controlled by PI controller with a set point of 343 K. Fig. 7 illustrates profiles of the time transient reactor and jacket water temperature for different cases.

At a higher initiator concentration with the same monomer concentration, the fluctuation of the reactor temperature and jacket water temperature took place earlier and more seriously (Fig. 7(a) and Fig. 7(b)). This can be explained in conjunction with Fig. 6(a). At a higher initiator concentration, the reaction rates become higher, which results in more heat of polymerization. The maximum reactor temperature for each case of M1, M2, M3, and M4 at 500 seconds is 346.7 K, 348.8 K, 349.5 K, and 350.1 K, while the jacket water temperature is close to the inlet temperature of chiller water (280.15 K). The slope of conversion curves starts reducing afterwards due to the reducing monomer concentration in polymerization. Hence, the reactor temperature and jacket water temperature get a smaller fluctuation and converge to a set point.

On the other hand, the higher initial monomer concentration under conditions of the same initiator concentration (Fig. 7(c) and

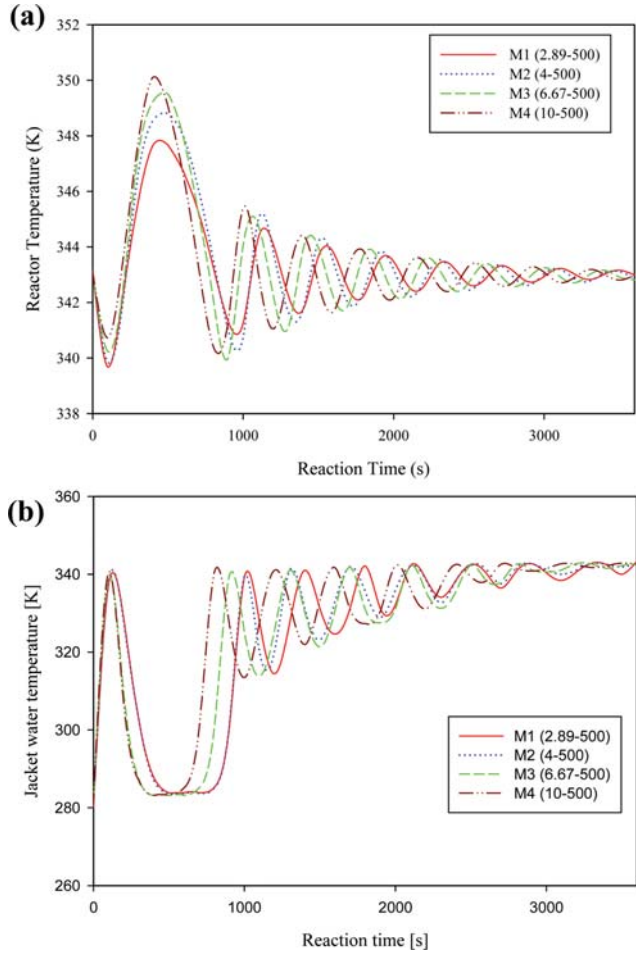

Fig. 7. Temperature profiles of the reactor and jacket water: (a)_reactor temperature for M1, M2, M3, and M4; (b)_jacket water temperature for M1, M2, M3, and M4; (c)_reactor temperature for I1, I2, I3, and I4 and (d)_jacket water temperature for I1, I2, I3, and I4.

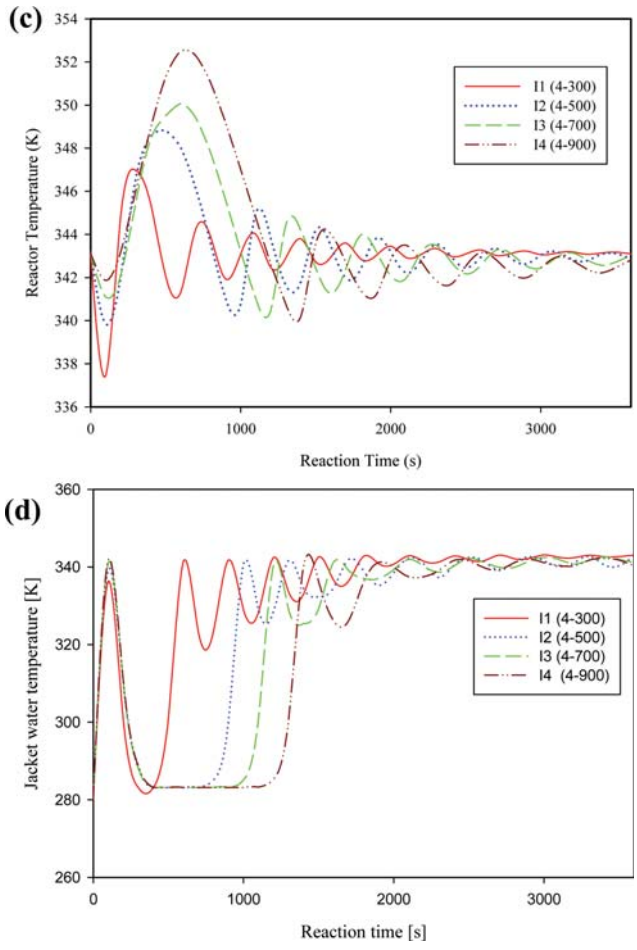

Fig. 8. Number average molecular weight profiles of polymer: (a) with fixed monomer and various initiator concentrations (M1, M2, M3, M4) and (b) with fixed initiator and various monomer concentrations (I1, I2, I3, I4).

Fig. 7(d)) creates much more radical polymer (R_1–R_n) [27]. Accordingly, conversion goes up more steeply and more heat is generated. As a result, temperature gets the maximum value for each case of I1, I2, I3, and I4 at 348 K, 348.8 K, 350.06 K, and 352.6 K after 350 s, 500 s, 600 s, and 620 s, respectively. At these states, jacket water temperature showed a value of 282.6 K, 283.15 K, 283.28 K, and 283.45 K for cases of I1, I2, I3, and I4. From these results, we acknowledge that the PI controller can control the reactor temperature around the set point value.

3. Polymer Properties

The four characteristic properties of polyacrylamide including Mn, Mw, MWD, and PD were calculated.

Fig. 8 shows the transient number average molecular weights (Mn) of polymer. In Fig. 8(a), as the initiator concentration increases, the conversion becomes faster as shown in Fig. 6(a). These results show the increasing of reaction rates as the initial monomer concentration is equal for all cases. Therefore, a higher initiator concentration generates a smaller polymer chain and gets a lower Mn. Also, in Fig. 8(b), as the monomer concentration is higher, the effect of the initiator is reduced, polymerization creates much more radical polymer as the higher conversion is achieved in Fig. 6(b). Thereby, the higher monomer concentration gets the higher Mn. This tendency agrees well with the results in the literature [27]. In all cases, Mn increases proportionately with conversion (Fig. 6) to get the peak and decreases slightly thereafter. This phenomenon is explained by the appearance of the large polymer chains that are produced at early times. The proportion of high molecular weight species is reduced as the conversion increases [19].

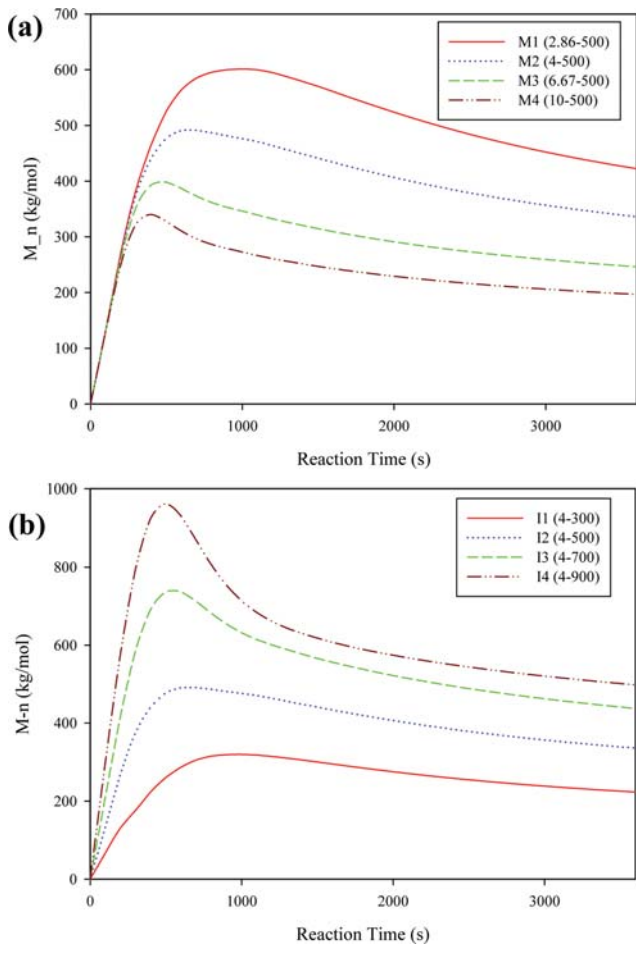

Fig. 9. Molecular weight distribution profiles of polymers: (a) with fixed monomer and various initiator concentrations (M1, M2, M3, M4) and (b) with fixed initiator and various monomer concentrations (I1, I2, I3, I4).

Fig. 9 shows the distribution of chain length with respect to weight fractions after 3,600 seconds of polymerization. Chain length is the number of monomers connected to form polymers, which consist of different number of chains, whereas the weight fraction of each chain length is the ratio between its weight and the total weight of polymer. Molecular weight distributions of the M1 and I4 cases (the lowest molar ratios of initiator and monomer) are broader than those of the M4 and I1 cases (the highest molar ratios of the initiator and monomer). This phenomenon is explained in conjunction with Fig. 6. The higher initiator concentration increases the decomposition and initiation rates, while the propagation and termination rates are also developed. So, the higher initiator concentration generates the smaller polymer chain and the narrower MWD as shown in Fig. 9(a). Likewise, in Fig. 9(b), the higher monomer concentration creates much more radical polymer and the molecular weight distribution is broadened. The tendency of the MWD curve is consistent with the results of another paper [12]. As shown in Table 6, the PD values are close to 2.0, which is the expected value for chain growth polymerization, whereas Mw values are in the range of results of the experiment paper [13]. Based on the simulation results, the desired product can be achieved with a cost saving for design of a commercial batch reactor by reducing the experiment. For application of water absorbent [28], a weight average molecular weight of 400 kg/mol and PD of 2 can be achieved with the concentration of AM at 500 mol/m^3 and I at 10 mol/m^3.

CONCLUSION

We performed process modeling and simulation of SAP production in a commercial scale batch reactor using acrylamide and potassium persulfate as reactant. The mathematical model included conservation equations, kinetic equations of polymerization, and heat transfer equation between reactor and cooling jacket. In our model, reactor temperature was controlled by model of cooling jacket using PI controller.

Table 6. Polymer properties after 3600 seconds for reaction

Case no.	Mn [kg/mol]	Mw [kg/mol]	PD
M1	422.25	840.73	1.991
M2	335.96	669.95	1.994
M3	246.19	491.12	1.995
M4	196.60	392.48	1.996
I1	223.36	445.84	1.996
I2	335.96	669.98	1.994
I3	437.61	872.04	1.992
I4	498.07	992.05	1.991

Parameter estimation to obtain kinetic parameter values with experimental reference data was performed. Developed mathematical model and experimental reference data were incorporated with the parameter estimation. These values were validated in terms of the conversion, average molecular weight, and molecular weight distribution of simulation result and reference data, and the maximum error was less than 10%.

Simulations of SAP were carried out through the case studies of different concentration ratios. The reaction time in the commercial scale of batch reactor could be reduced with increasing the reactant concentration, and the number average molecular weight could increase from 196.6 to 498.7 kg/mol but still keep the PD values, which were close to 2.0 (expected value).

Finally, the methodology and results of this research can be used to scale up the batch reactor of acrylamide polymerization in the early stage of design.

NOMENCLATURE

Symbol

A_t : area of tube [m^2]
$A_{h,t}$: heat transfer area [m^2]
C_s : bias signal [kg/s]
c_i : concentration of component i [mol/m^3]
c_i^p : concentration of polymer i [mol/m^3]
c_{total}^p : total concentration of polymer [Mol/m^3]
$\hat{c}_p$: heat capacity [J/(kg K)]
$\hat{c}_{p,c}$: heat capacity of water [J/(kg K)]
D : decomposition
E : activation energy [J/mol]
h : heat transfer coefficient [$J/(m^2\ s\ K)$]
$\hat{h}_c^{in}$: enthalpy of water at inlet of cooling jacket [J/kg]
$\hat{h}_c^{out}$: enthalpy of water at outlet of cooling jacket [J/kg]
h_P : heat of polymerization [J/mol]
I : initiation
k : rate constant [$m^3/(mol\ s)$]
k_d : heat conductivity of reactor [J/(m s K)]
k_0 : frequency factor
L : height of reactor
m : mass [kg]
$\dot{m}_c^{in}$: mass flow rate at inlet of cooling jacket [kg/s]
$\dot{m}_c^{out}$: mass flow rate at outlet of cooling jacket [kg/s]
M : monomer
M_i : molecular weight of i^{th} polymer [kg/mol]
M_n : number average molecular weight [kg/mol]
M_w : weight average molecular weight [kg/mol]
N : total number of measurements
NE : number of experiments performed
NM_{ij} : number of measurement of j^{th} variable in the i^{th} experiment
P : propagation
K_c : proportional gain
PD : polydispersity
$\dot{q}$: heat of transfer with cooling jacket [J/s]
R : ideal gas constant [J/(mol K)]
R_t : total resistance [(K s)/J]
R_t^{cond} : resistance of conduction [(K s)/J]
R_t^{conv} : resistance of convection [(K s)/J]
r : radius of reactor [m]
r_c : radius of cooling jacket [m]
r_J : reaction rate of reaction J [$mol/m^3 s$]
r_J^i : reaction rate of the i^{th} component in reaction J [mol/m^3-s]
$\hat{s}_e$: energy source from reaction of polymerization [$J/(m^3 s)$]
$\hat{s}_m^i$: mass source from reaction of component i [$mol/(m^3 s)$]
T : termination
T_R : reactor temperature [K]
T_c : temperature in cooling jacket [K]
T_l : lowest limit of reactor temperature [K]
T_h : highest limit of reactor temperature [K]
T_{SP} : highest limit of reactor temperature [K]
U : overall heat transfer coefficient [$J/(m^2 sK)$]
v : volume of reactor [m^3]
X : conversion
$\tilde{X}_{ij}$: j^{th} measured value of conversion in experiment i
X_{ij} : j^{th} (model-)predicted value of conversion in experiment i

Greek Symbols

ρ : density [kg/m]
τ_I : reset time of integral time constant [1/s]
ε : error [K]
ω : constant standard deviation
θ : set of parameters
σ_{ij} : variance of the j^{th} measurement of conversion in experiment i^{th}
γ_{ji} : stoichiometric coefficient of component i in reaction J

REFERENCES

1. S. Francis, M. Kumar and L. Varshney, *Radiat. Phys. Chem.*, **69**, 481 (2014).
2. S. C. Chang, J. S. Yoo, J. W. Woo and J. S. Choi, *Korean J. Chem. Eng.*, **16**, 581 (1999).
3. R. E. Sojka and J. A. Entry, *Environ. Pollut.*, **108**, 405 (2000).
4. J. Z. Mohammad and K. Kabiri, *Iran. Polym. J.*, **17**, 451 (2008).
5. M. Wisniewska, S. Chibowski and T. Urban, *J. Ind. Eng. Chem.*, **21**, 925 (2015).
6. G. Sodeifian, R. Daroughegi and J. Aalaie, *Korean J. Chem. Eng.*, **32**, 2484 (2015).
7. D. Chamovsk, M. Cvetkovska and T. Grchev, *Croat. Chem. Acta*, **81**, 461 (2008).
8. A. Pourjavadi and G. R. Mahdavinia, *Turk. J. Chem.*, **30**, 595 (2006).
9. A. A. Oladipo, *Synthesis and characterization of modified chitosan-based novel superabsorbent hydrogel: swelling and dye adsorption behavior*, Master's Thesis EMU (2011).
10. M. Sadeghi and H. Hosseinzadeh, *Turk. J. Chem.*, **32**, 375 (2008).
11. R. A. Scott and N. A. Peppas, *AIChE J.*, **43**, 135 (1996).
12. T. Ishige and A. E. Hamielec, *J. Appl. Polym. Sci.*, **17**, 1479 (1973).
13. A. Giz, H. C. Giz, A. Alb, J. L. Brousseau and W. F. Reed, *Macromolecules*, **34**, 1180 (2001).
14. D. Hunkeler, *Macromolecules*, **24**, 2160 (1991).
15. C. Preusser, A. Chovancova, I. Lacik and R. A. Hutchinson, *Macromol. React. Eng.*, **10**, 490 (2016).
16. Process Systems Enterprise Co., https://www.psenterprise.com

(2017).
17. N. D. Vo, M. Y. Jung, D. H. Oh, J. S. Park, I. Moon and M. Oh, *Combust. Flame*, **189**, 12 (2018).
18. S. H. Kim, B. W. Nyande, H. S. Kim, J. S. Park, W. J. Lee and M. Oh, *J. Hazard. Mater.*, **308**, 120 (2016).
19. K. Venkatarao and M. Santappa, *J. Polym. Sci.*, **8**, 1785 (1970).
20. N. Y. Abu-Thabit, *World J. Chem. Education*, **5**, 94 (2017).
21. A. Echtermeyer, Y. Amar, J. Zakrzewski and A. Lapkin, *Beilstein. J. Org. Chem.*, **13**, 150 (2017).
22. H. R. Lin, *Eur. Polym. J.*, **37**, 1507 (2001).
23. I. Rintoul and C. Wandrey, *Lat. Am. Appl. Res.*, **40**, 365 (2010).
24. S. C. Kang, Y. J. Choi, H. Z. Kim, J. B. Kyong and D. K. Kim, *Macromol. Res.*, **12**, 107 (2004).
25. P. Pladis, O. Kotrotsiou, C. Gkementzoglou and C. Kiparissides, *A Comprehensive Kinetic Investigation of the Inverse Suspension Copolymerization of Acrylamide: Theoretical and Experimental Studies*, 2015 10th Int. Conf. Panhellenic Scientific Conference in Chemical Engineering (2015).
26. Z. Abdollahi and V. G. Gomes, *Synthesis and characterization of polyacrylamide with controlled molar weight*, Chemeca 2011: Engineering a Better World (2011).
27. J. Xu, W. P. Zhao, C. X. Wang and Y. M. Wu, *Express. Polym. Lett.*, **4**, 275 (2010).
28. Sigma-aldrich Co., https://www.sigmaaldrich.com/catalog/product/aldrich/767379?lang=ko&region=KR&cm_sp=Insite-_-prodRecCold_xviews-_-prodRecCold10-1 (2018).